3D Numerical Simulations of Eruption Cloud Dynamics and Tephra Dispersal

Project Representative

Takehiro Koyaguchi   Earthquake Research Institute, The University of Tokyo

Authors

Yujiro Suzuki   Earthquake Research Institute, The University of Tokyo

Takehiro Koyaguchi   Earthquake Research Institute, The University of Tokyo

We are developing a three-dimensional (3D) numerical model that reproduces the formation of volcanic plume, the tephra dispersal in the atmosphere and the deposition of tephra on the ground under various wind conditions. We have carried out simulations for two extreme cases: a weak plume in a strong wind field and a strong plume in a weak wind field. When the magma discharge rate is low and the wind speed in the atmosphere is high, the mixture of the volcanic gas and solid pyroclasts ejected from the vent is largely distorted by the wind. The tephra particles drift leeward at the neutral buoyancy level (NBL) where the cloud density is equal to the atmospheric density; as a result, the dispersal axis of main tephra fall deposits extends leeward. On the other hand, if the magma discharge rate is high and the wind speed is slow, the eruption cloud (the mixture of the ejected material and entrained air) rises almost vertically and forms a concentric umbrella cloud at the NBL. The tephra particles are transported radially and deposit in both leeward and windward regions. In this case, the distribution of fall deposits slightly elongates in the downwind direction owing to the wind effect. On the basis of the simulation results, the distribution of number density of marker particles and the size distribution on the ground are obtained. These distributions can be compared with the isomass and isopleth maps based on field observations.

Keywords: volcanic eruption, eruption column, ash dispersal, volcanic hazard

1. Introduction

Explosive volcanic eruptions can cause a widespread tephra dispersal. During explosive eruptions, a mixture of solid particles (pyroclasts) and volcanic gas is ejected from vents into the atmosphere. As the ejected material entrains ambient air by turbulent mixing, the entrained air expands rapidly owing to the heating from the hot pyroclasts. Consequently, the density of the cloud (i.e., the mixture of the ejected material and the entrained air) becomes lower than the atmospheric density and forms buoyant plume [1, 2]. The eruption cloud exhausts its thermal energy and loses its buoyancy within the stratified atmosphere. At the level where the cloud density is equal to that of the atmosphere (i.e., NBL), the eruption cloud spreads laterally. Tephra particles are lifted upward by buoyant plume and transported by laterally-spreading cloud.

The flow patterns of eruption cloud, and hence, the depositional patterns of tephra particles are controlled by the intensity of eruption and the strength of the atmospheric wind [3, 4]. At high eruption intensities and/or under weak wind speeds, plume trajectories are not wind-affected. In this case, a plume rises vertically, and subsequently it spreads radially as an umbrella cloud at the NBL. Tephra particles are separated from the vertically-rising plume or radially-spreading cloud; as

a result, the tephra particles are distributed concentrically on the ground. In contrast, if eruption intensity is weak and/or wind speeds are high, volcanic plumes are highly distorted by the wind, leading to a bent-over trajectory. In this case, the tephra particles can be transported leeward and its depositional area can significantly deviate from concentric distribution.

Recent progress has been made on developing a more quantitative understanding of the wind-effects on the depositional patterns of tephra particles [e.g., 5]. However, in these studies, the distributions of tephra particles in eruption clouds are given as an initial conditions on the basis of one-dimensional models of volcanic plume [6, 7]. We attempt to directly simulate the motion of tephra particles ejected from the vent in the atmosphere and their deposits on the ground using a 3D numerical model.

2. Numerical model

Our numerical model is designed to simulate the behavior of a gas-particle mixture ejected into the stratified atmosphere with one-way coupling between fluid and particle motions [8]: marker particles do not have any effect on the fluid, whereas the particle motion depends on the fluid motion. During fluid dynamics calculations, we ignore the separation of solid

pyroclasts from the eruption cloud, treating an eruption cloud as a single gas with a density calculated using a mixing ratio between ejected material and entrained air [9]. The governing equations are solved numerically by a general scheme for compressible flow. For the calculations of particle motion, our model employs Lagrangian marker particles of ideal sphere. The density of particles is assumed to be $1000 - 2500$ kg m^{-3}, and about 200 marker particles are ejected from the vent every 2 sec at the same velocity as the pseudo-gas. Particle grain sizes are randomly selected within a range of 0.0625 to 64 mm. The terminal velocity is added to the vertical velocity of fluid motion at every time step, until the marker particle ceases its motion and settles as sediment when it reaches the ground surface.

3. Simulation results

In order to understand the wind-effects on the tephra dispersal, we carried out numerical simulations for two cases: a weak plume in a strong wind field and a strong plume in a weak wind field.

3.1 Weak plume in strong wind field

Magma discharge rate is set to be 2.5×10^6 kg s^{-1}. The speed of horizontal wind linearly increases with height, reaching 80 m s^{-1} at $Z = 10$ km. The wind speed is assumed to be horizontally uniform at each height, with vertical wind velocity assumed to be zero. The volatile content (H$_2$O) and magma temperature are 2.84 wt% and 1000 K, respectively. The mid-latitude atmosphere is applied to calculate the atmospheric density, pressure, and temperature.

A computational domain extends 13 km vertically (Z–direction) and 30 km × 12 km horizontally (X– and Y–directions, respectively). The boundaries are located at $X = -3$, 27 km (YZ – plane) and $Y = -6$, 6 km (XZ – plane). Grid sizes are set to be $D_0/16$ near the vent, where D_0 is the vent diameter, and to increase at a constant rate (by a factor of 1.02) with distance from the vent up to $D_0/2$.

Our simulation successfully reproduced fundamental features of typical weak plumes in the strong wind fields (Fig. 1). The plume near the vent is largely distorted by wind. A distal horizontally moving cloud develops at the NBL (6 – 8 km a.s.l.). Our simulations also reproduce particle separation and sedimentation from the volcanic plume (Fig. 1c). The marker particles ejected from the vent are lifted upward by the bent-over plume, and leave from the cloud because their density is higher than that of the gas phases. Fine particles (shown by red points) are transported to the top of the plume, are carried by the horizontally moving cloud, and spread leeward. In contrast, coarse particles (blue points) leave from the volcanic plume and fall to the ground near the vent. Medium-sized particles (light blue points) show intermediate features between the fine and coarse particles; they are lifted up to higher level than the coarse particles, but do not reach the top of the plume.

On the basis of the simulation results of marker particles settled on the ground, we obtain the distribution of tephra deposits (Fig. 2a) and their particle size distribution (Fig. 2b). The results show the general features that the dispersal axis of main fall deposits extends leeward and that the number and the maximum size of particles decreases with distance from the vent.

3.2 Strong plume in weak wind field

Magma discharge rate is set to be 1.0×10^9 kg s^{-1}. The speed of horizontal wind is given as $U_{wind} = 15\tanh(Z/1000)$ m s^{-1}. The volatile content (H$_2$O) and magma temperature are 4 wt% and 1053 K, respectively. The tropical atmosphere is applied to calculate the atmospheric density, pressure, and temperature.

A computational domain extends 58 km vertically (Z-direction) and 456 km × 456 km horizontally (X- and Y-directions, respectively). The boundaries are located at $X = -192$, 264 km (YZ – plane) and $Y = -228$, 228 km (XZ – plane). Grid sizes is set to be $D_0/20$ near the vent, and to increase at a constant rate with distance from the vent up to 300 m.

Typical features of the developments of an eruption column and an umbrella cloud in the weak wind field are reproduced in the present simulation (Fig. 3). The buoyant plume rises vertically and is not largely affected by wind. The plume overshoots the NBL (20 – 25 km) and reaches the height of 40 km. The umbrella cloud at the NBL spreads radially with diameter of ~400 km at 5500 s. The center of the umbrella cloud is located at 40 km leeward from the vent, which approximately coincides with the position of the maximum height. Pattern of ash dispersion is different from that from the weak plume ejected in the strong wind field (Fig. 3c). Fine particles (shown by red points) are transported radially by the umbrella cloud, whereas coarse particles (blue points) leave from the volcanic plume near the vent. Medium-sized particles (light blue, yellow, and orange points) separate from the umbrella cloud. Between the umbrella cloud and the ground, all the particles are drifted leeward by the wind to considerable extent.

The distribution of number density of marker particles (Fig. 4a) and the size distribution (Fig. 4b) on the ground show that the particles are dispersed almost concentrically. However, the distribution of fall deposits slightly elongates in the downwind direction.

4. Concluding remarks

We have developed a 3D numerical model of volcanic plumes in wind fields to simulate the dispersal and deposition of volcanic ash particles. The present model can reproduce the typical features of flow patterns of eruption cloud such as buoyant plume distorted by strong wind, umbrella cloud drifted by weak wind, and those of tephra deposits. The distribution of number density of marker particles settled on the ground can be compared with the isomass map based on field observations. In

addition, the size distribution of marker particles on the ground can be directly compared with the isopleth map based on field observations. The present model is considered to be useful for quantitative analyses of eruption cloud observations and geological data of tephra deposits in the future.
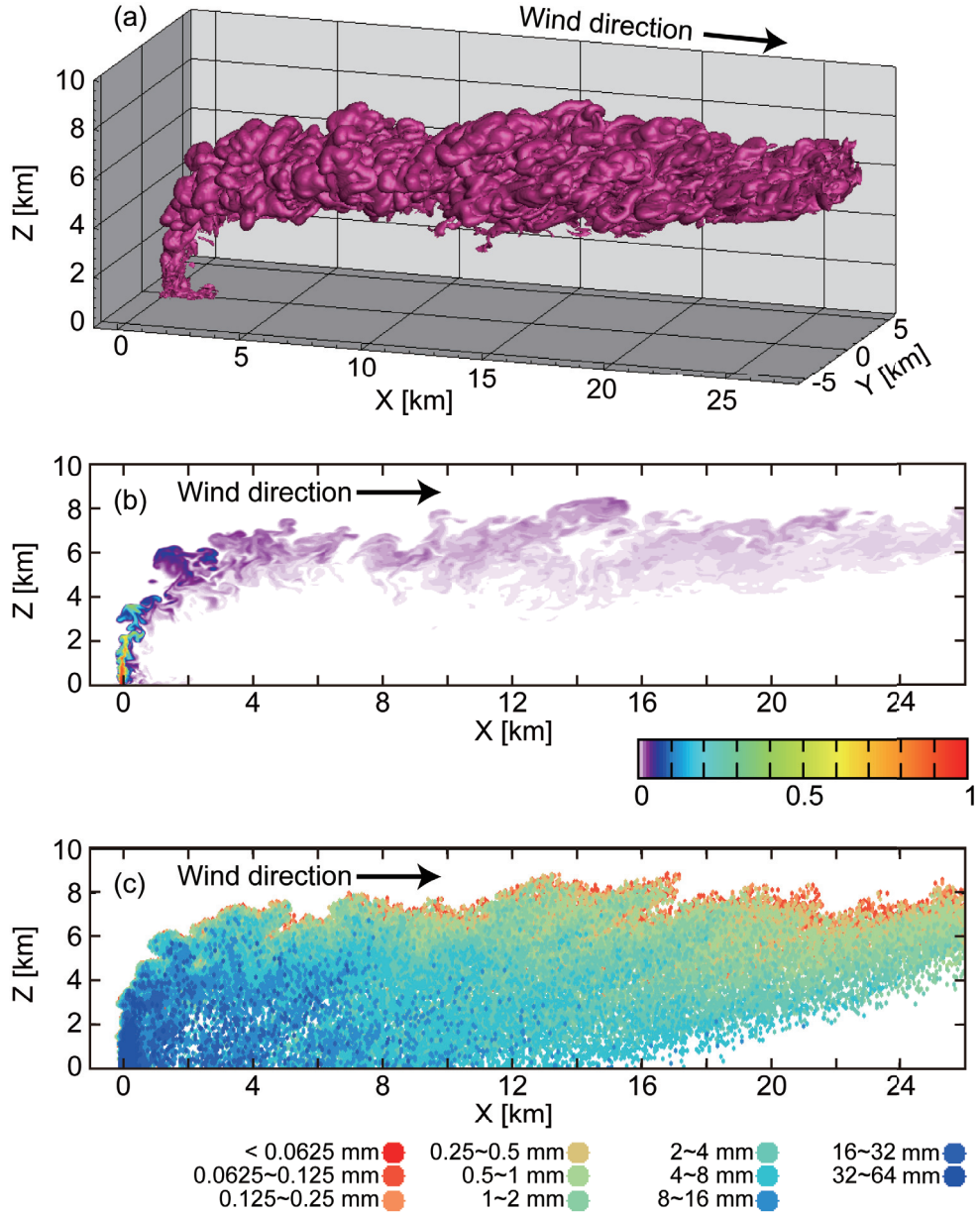

Fig.1 Results of 3D numerical simulation of a weak volcanic plume distorted by a strong wind at 700 s from eruption initiation. The wind blows rightward (for the wind profile see text). (a) Bird-eye view of the iso-surface of $\xi = 0.02$, where ξ is the mass fraction of the ejected material. (b) Cross-sectional distribution of ξ in X–Z space. (c) Side view of the distribution of marker particles. The colors in (c) represent the size of marker particles.
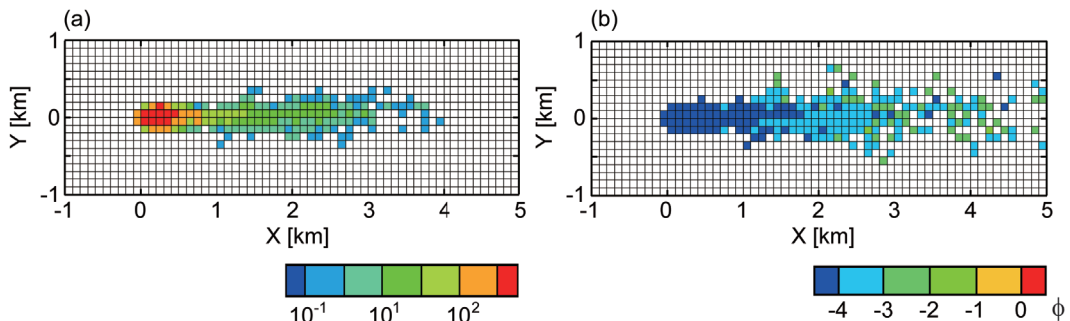

Fig.2 Depositional patterns of marker particles separated from a weak plume in a strong wind field. (a) The distribution of number density of marker particles at 700 s from the eruption initiation. (b) The distribution of maximum size of marker particles at 700 s from the eruption initiation.
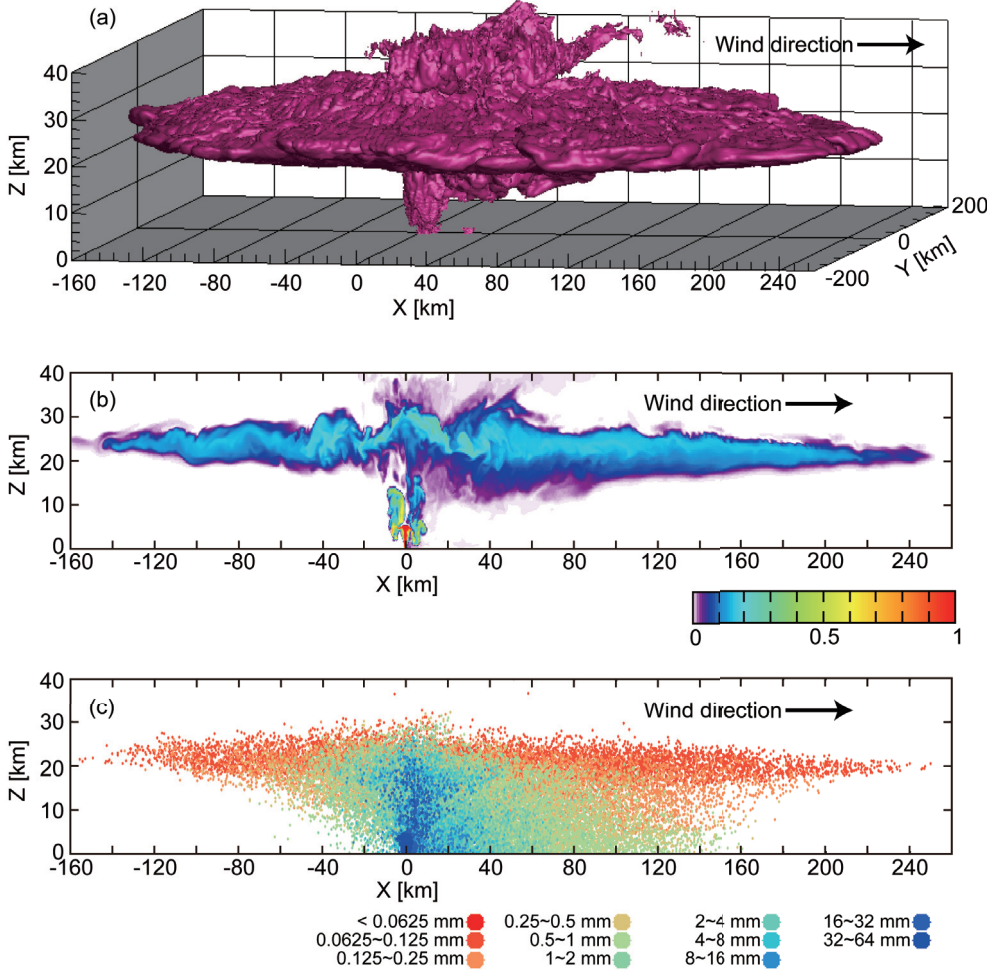
Fig.3 Results of 3D numerical simulation of a strong volcanic plume distorted by a weak wind at 5500 s from eruption initiation. The wind blows rightward (for the wind profile see text). (a) Bird-eye view of the iso-surface of $\xi = 0.02$. (b) Cross-sectional distribution of ξ in X–Z space. (c) Side view of the distribution of marker particles. The colors in (c) represent the size of marker particles.
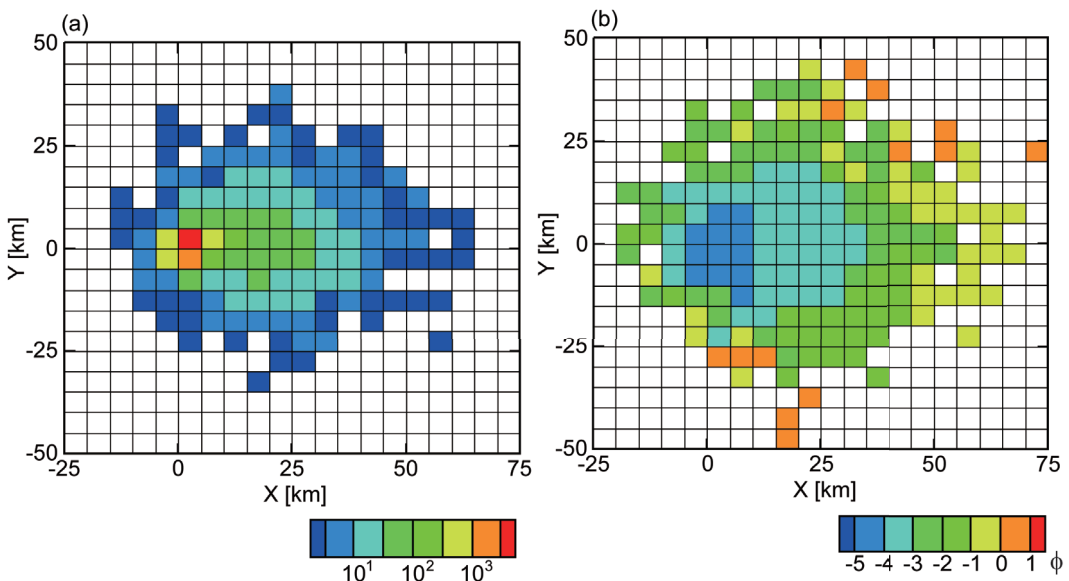

Fig.4 Depositional patterns of marker particles separated from a strong plume in a weak wind field. (a) The distribution of number density of marker particles at 5500 s from the eruption initiation. (b) The distribution of maximum size of marker particles at 5500 s from the eruption initiation.

References

[1] B. R. Morton, G. Taylor, and J. S. Turner, "Turbulent gravitational convection from maintained and instantaneous sources", Proc. R. Soc. Lond. A, vol.234, pp.1-23, 1956.

[2] R. S. J. Sparks, "The dimensions and dynamics of volcanic eruption columns", Bull. Volcanol, vol.48, pp.3-15, 1986.

[3] C. Bonadonna, J. C. Phillips, and B. F. Houghton, "Modeling tephra sedimentation from a Ruapehu weak plume eruption", J. Geophys. Res., vol.110, B08209, 2005.

[4] S. Carey and R. S. J. Sparks, "Quantitative models of the fallout and dispersal of tephra from volcanic eruption columns", Bull. Volcanol., vol.48, pp.109-125, 1986.

[5] A. Costa, G. Macedonio, and A. Folch, "A three-dimensional Eulerian model for transport and deposition of volcanic ashes", Earth Planet. Sci. Lett., vol.241, pp.634-647, 2006.

[6] M. Bursik, "Effect of wind on the rise height of volcanic plumes", Geophys. Res. Lett., vol.28, no.18, pp.3621-3624, 2001.

[7] A. W. Woods, "The fluid dynamics and thermodynamics of eruption columns", Bull. Volcanol., vol.50, pp.169-193, 1988.

[8] Y. J. Suzuki and T. Koyaguchi, "3D numerical simulation of volcanic eruption clouds during the 2011 Shinmoe-dake eruptions", Earth Planets Space, vol.65, pp.581-589, 2013.

[9] Y. J. Suzuki, T. Koyaguchi, M. Ogawa, and I. Hachisu, "A numerical study of turbulent mixing in eruption clouds using a three-dimensional fluid dynamics model", J. Geophys. Res., vol.110, B08201, 2005.

火山灰輸送・堆積の３次元数値シミュレーション

課題責任者

小屋口剛博　　東京大学　地震研究所

著者

鈴木雄治郎　　東京大学　地震研究所

小屋口剛博　　東京大学　地震研究所

　本プロジェクトでは、固体地球と地球表層・大気にまたがる火山現象について、大規模数値シミュレーションを用いた物理過程の理解と計算結果の防災への応用を目指している。特に、火山噴煙の到達高度や火山灰の降灰分布を定量的に正しく再現することに焦点をあて、噴煙ダイナミクスを支配する乱流混合や流体中の固体粒子沈降などの素過程の理解を進めている。

　爆発的火山噴火では、高温の火山灰（マグマの破片）が水蒸気を主体とする火山ガスと混合した状態で火口から大気中へと噴出する。噴出した火山灰・ガスの混合物は、周囲の大気を取り込んで膨張させることで浮力を獲得して噴煙柱を形成する。成層大気中で噴煙（噴出物と混合大気の混合物）の密度と大気密度が釣り合うと、噴煙はその密度中立高度で水平方向へと拡大する。火山灰はこの噴煙上昇と水平移動によって運搬されるが、その輸送・堆積パターンは風の影響を受ける。平成 25 年度は、火山灰の移動を含めた噴煙の 3 次元数値シミュレーションを行い、火山灰輸送・堆積パターンへの風の影響を調べた。特に、（a）風が強い大気中での弱い噴火、（b）風が弱い大気中での強い噴火、の 2 種類の場合について、噴煙挙動と火山灰輸送・堆積過程を比較した。

（a）風が強い大気中での弱い噴火は、新燃岳 2011 年噴火程度の噴火強度を想定し、噴出率を 2.5×10^6 kg s^{-1} とするシミュレーションを行った。大気中の風については、地表で 0 m s^{-1}、高度 10 km で 80 m s^{-1} まで高さとともに風速が直線的に増加する初期プロファイルを与えた。シミュレーションの結果、噴煙は風下方向に大きく曲がり、密度中立となる高度 6 〜 8 km で水平に流れた。火山灰はこの噴煙によって運搬され、風下側のみに堆積した。火山灰の輸送・堆積パターンは、粒子サイズによって大きく異なった。数 cm サイズの粒子は上昇中の噴煙柱から分離し、火口付近に堆積した。数 mm 〜 1cm サイズの粒子は噴煙柱上昇によって噴煙上部まで到達し、密度中立高度で噴煙とともに水平に移動するが、その後、水平移動する噴煙から徐々に分離して地表面へと降下した。非常に細かな粒子は噴煙から分離せず、水平移動する噴煙内を移動し続けた。

（b）風が弱い大気中での強い噴火は、ピナツボ 1991 年噴火程度の噴火強度を想定し、噴出率を 1.0×10^9 kg s^{-1} とするシミュレーションを行った。大気中の風速については、高度 Z に対し、$U_{wind} = 15\tanh(Z/1000)$ m s^{-1} で与えた。シミュレーションの結果、噴煙柱は風の影響をほとんど受けずに鉛直方向に上昇し、密度中立高度でほぼ同心円状に拡大し、傘型噴煙を形成した。シミュレーション結果では、この傘型噴煙の中心が、風の影響で火口直上から風下側に徐々に移動する様子が観察された。火山灰は、同心円上に拡大する傘型噴煙から降下・分離し、風下側・風上側の両方に堆積するが、その分布は風の影響で風下側に偏向する。

　以上のように、火山灰輸送と堆積に対する風の影響を定性的に捉えることができた。また、シミュレーション結果から地表における粒子密度分布と粒子サイズ分布を作成することができ、これらは実際の火山噴火における地質調査によって作成される堆積分布図と比較・検証することが可能である。

キーワード：火山噴煙，降灰分布，火山災害